The Research on the Microscopic Mechanism and Dynamical Characteristics of DC Positive Corona Discharge in Pure O$_2$

JIAN SUI[1,2], PANLONG AN[3], AND ZHENGGUANG LIU[4]

[1]State Key Laboratory of Power Transmission Equipment and System Security and New Technology, Chongqing University, Chongqing 400044, China
[2]Oceanography College, Shanwei Polytechnic, Shanwei 516600, China
[3]Shaanxi Railway Institute, Weinan 714000, China
[4]Department of Public Basis, Zhaoqing Medical College, Zhaoqing 526020, China

Corresponding author: Jian Sui (weilaihao_sj1@163.com)

ABSTRACT We systematically research the microscopic physical mechanism of positive corona discharge and comprehensively analyse the regular and irregular pulsed oscillations of discharge outputs. Especially, we discover the formation mechanism of irregular pulsed discharge phenomenon for the positive corona and give a profound explanation. According to the physical process of discharge, we propose a new dynamical model which can describe the Trichel pulsed discharge outputs and the characteristics of waveforms. Based on nonlinear dynamics method, we predict and analyse different stages of discharge. In particular, the experimentally observed irregularly pulsed discharge on positive corona is reproduced by the presented theory. Our study reveals that the positive ions as current carriers predominate in the total current and the photons occurring can be treated as the feedback signal in the nonlinear process of discharge system. We find that the photo-ionization is an indispensable role as the source forming electron avalanches for sustaining the positive corona discharge. Moreover, according to quantum mechanics we demonstrate the high frequency photons with energy higher than the ionization energy may photo-ionize oxygen molecules in pure oxygen. We point out that the recombination radiation is competent to photo-ionize neutral molecules producing the seed electrons. Besides, we analyze the characteristics of diversely pulsed outputs and further explain the microscopic mechanism generating the symmetric and asymmetric sharp jagged pulses. Furthermore, we discover the intrinsic physical relations between positive ion and surface electric field, and the significant influences of the attributes of different particles on the discharge behaviors.

INDEX TERMS Chaos, high frequency radiation, nonlinear coupled oscillator, photo-ionization, recombination, Trichel pulse, positive ions.

I. INTRODUCTION

In 1838, Faraday [1] first observed and recorded the phenomenon of positive corona discharge at atmospheric pressure. Until 1939, Trichel [2] thoroughly researched on the positive corona discharge in the point-to-plane configuration, which showed a series of irregular current-pulses and a visual glow in the positive corona discharge. This sort of pulse in corona discharge was named as 'Trichel pulse' [3]. From then

on, the studies on the properties of a glow positive corona began catching a lot of interests of researchers. Experimentally, W. N. English observed the corona pulse and made a careful comparison of positive and negative corona [4]. Lama and Gallo [5] performed a comprehensively detailed research on Trichel pulses in air and figured out a connection between the average current and the pulsed frequency, and drew some empirical formulas. It is found that with the voltage increasing the Trichel pulsed frequency is higher and meanwhile that the Trichel pulsed frequency is a quadratic functional dependence of the

The associate editor coordinating the review of this manuscript and approving it for publication was Lin Zhu.

applied voltages and there also exists an inversely proportional relationship between the Trichel pulsed frequency and the square of electrode interval and electrode radius. The results of Mayoux and Goldman [6] investigation show that the electrically induced pulses and photon pulses have a correspondence between electrical and luminous phenomena for positive pulses. Besides, Ferreira *et al.* [7] developed the empirical formulas of current-voltage characteristics for both positive and negative coronas. V. Brunt *et al.* figured out that the pulsed discharge appears in the positive and negative corona in SF_6 gas [8]. In the research of Ono *et al.* [9], the effect of pulse width on the production of active species is studied in a pulsed positive corona discharge. It is shown that the discharge pulse can be divided into three phases related to the production of active species. Meanwhile, in the work of Denholm and Rakoshdas the dynamic characteristics of positive corona on peak value and pulse rate is investigated [10], [11].

Sarma *et al.* [12] theoretically investigated in a cylindrical configuration a d.c. discharge of stationary-state on the positive and negative corona according to the Townsend theory. In the research of Giao and Jordan [13], it is found that there is the electrical current of pulsative form in the positive corona discharge. However, for the prior reports of positive corona discharge, the most work concentrated on either the experimental observations and measurements or the theoretical analysis of stationary-state discharge. Noticeably, in 1997 a detailed numerically computing study on the positive corona was implemented by Morrow [14]. In his theory, for the concentric-sphere electrode in air the current and light pulses of positive corona are shown under a DC current level. Furthermore his model can predict that the current and the surface electric field have 'saw-toothed' pulsed form respectively and vary with applied voltage. Meanwhile, during the pulse discharge the most of the mean current is carried by positive ions, and photo-ionization is crucial for the avalanches at the anode. Furthermore, these numerically computing results are in excellent agreement with the available experimental observations. In addition, Akishev *et al.* [15] studied the oscillatory behavior of a glow positive corona in pure N_2 and presented a corresponding numerical model. It is revealed that the positive glow corona generates a soft x-radiation which plays an important role in the photo-ionization of N_2.

Currently, lots of researches are usually focused on the numerical simulation [16]–[20], [25], which simulated a series of Trichel pulses for different applied voltages and showed the frequency of Trichel pulses changing with the increase of the applied voltage. In meantime, in the past studies on the output of oscillations [14], [21], it is revealed that the current and luminosity of the glow positive corona are oscillated regularly with a high frequency. It is found that a waveform of the current self-oscillations have a relaxation type with a sharp increase of rising edge of the current pulse and a slow decay of falling edge. It is also figured out that the waveform of a light emission signal is more symmetric. Generally speaking, these researches discover some dynamic

natures of positive corona discharge. However the previous implemented theoretical investigations are concerned only with the periodic pulsed and stationary discharge of positive corona, and they cannot still very precisely reflect the actual discharge situation in the positive glow corona discharge. The actual discharge of positive corona has the irregular pulses and the chaotic characteristics, which are observed in the experimental researches [2], [22]. In the meantime, although the chaotically dynamic characteristics are important phenomena in the positive corona discharge, the most of these researchers are interested only in the stably positive corona discharges and their applications, and neglect the chaotically dynamic characteristics. Especially for the recent years, researchers put a lot of attentions on computing software and implementing methods, and however so far they rarely fulfilled deeper explorations on the inherent physical principle of discharge. These situations reflect that the dynamic mechanism of positive corona has been not still found adequately and meanwhile the principle governing the chaotic discharge needs to be revealed.

The photo-ionization has a key position in the positive corona discharge, which is found to be significant during the period of discharge for maintaining self-sustained discharge of positive corona. An experimental research was carried out by Penney *et al.* [23] to measure the photo-ionization under the different pressure in the air. In R. Morrow's theory, it is supposed that the photo-ionizing radiation is generated near the central electrode and moves outwards radially, ionizing the molecules to produce the seed electrons. In the results of Akishev *et al.* [15], it is believed that the bremsstrahlung x-ray radiation is the versatile and most important ionizing agent in a positive corona. Besides, Naidis [24] investigated the photo-ionization phenomenon in the dry and moist air and indicated that the absorption of radiation by water molecules is essential to simulate photo-ionization in moist air. However, heretofore the microscopic mechanism of photo-ionization for the positive corona discharge has not been clearly clarified yet.

In contrast to the negative corona discharge, the theoretical studies on the pulsed discharge of positive corona are still fewer. The researches of positive corona discharge are mainly about experiments and numerical simulations. So far the actual positive corona discharge which has the nature of non-repetitively pulsed outputs is not given an adequately dynamic description and theoretically explained. Additionally, although lots of earlier researches mention the process of photo-ionization on positive corona, the inherent physical mechanism causing photo-ionization isn't definitely demonstrated and only a vague concept of photons ionizing neutral molecules is given. Besides, the influence of radiated photons on the process of discharge is not discovered clearly. These issues are vital to the positive corona discharge, and thus they are necessary to be further in depth explored.

At present, there is a lack of the researches on the aperiodic phenomenon and microscopic mechanism in the positive corona discharge. In our research, we systematically investigate the discharge process of positive corona and the

discharge natures. Furthermore, we study the microscopic physical mechanism of positive corona discharge and the importance of photo-ionization, and we extensively analyse the variation of discharge outputs with time. In the meantime, we propose a novel dynamical model predicting different stages of discharge including the stationary-state discharge, the periodic pulse discharge and the chaotic pulse discharge. In addition, by the analysis of nonlinear time series, we focus on the characteristics of corona discharge with the evolution of time and theoretically realize the chaotic oscillation of Trichel pulse on positive corona. Especially, compared with previous researches we figure out the dynamical mechanism producing chaotic phenomenon for the positive corona discharge and give a physical explanation.

II. PHYSICAL PROCESS AND DYNAMIC MODEL

In our work, the system of discharge is composed of the concentric-sphere electrode system structure, as shown in Fig. 1. Near the inner electrode, the system of positive corona discharges very intensively compared with other area in the system and a stably high positive voltage is applied to the electrode of discharge. The discharging area is a plasma region including the distribution of various particles such as electrons, positive ions, negative ions and photons. In order to analyze conveniently and grab on the essential issues, the region of discharge near the anode is considered and only the electrons, positive ions, negative ions and photons are assumed to participate in the process of discharge. In addition, Fig. 2 shows the equivalent circuit of discharge system including the discharge electrodes, the effective capacitor, the equivalent resistance and the power offering control voltage.
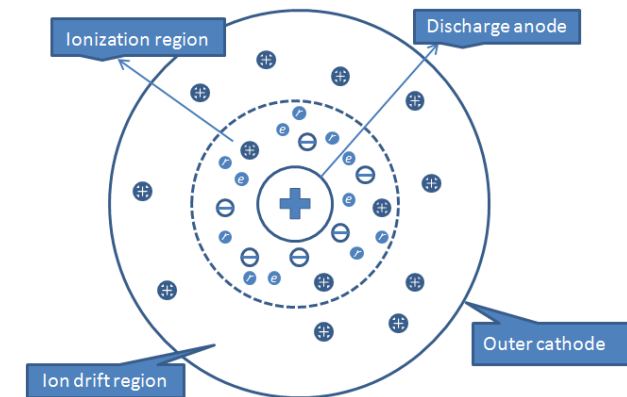

FIGURE 1. Schematic diagram of positive corona discharge for concentric-sphere electrode system.

A. THE DISCUSSION OF PHYSICAL MECHANISM OF DISCHARGE

The photo-ionization is very important in the positive corona discharge and often studied in many literatures, which is a key factor for sustaining discharge. Although lots of earlier researches mention the process of photo-ionization on positive corona, these literatures don't definitely demonstrate
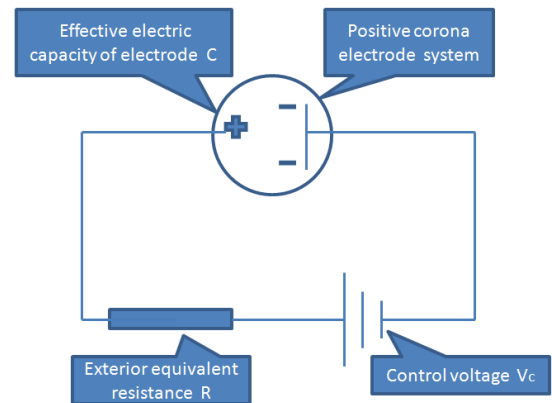

FIGURE 2. Schematic diagram of equivalent circuit of positive corona: C is the effective capacitor, R is the equivalent resistance and V_c is the control voltage.

the source of photons which are capable to ionize neutral molecules and only account for an ambiguous concept of photons ionizing neutral molecules. Thus we need to further deeply investigate the physical mechanism producing photons and figure out the source of photons ionizing O_2 molecules.

Considering that photons need to ionize O_2 molecules producing secondary electrons as seed electrons, we analyze two sources producing photons including the excitation radiation and recombination radiation.

Firstly, because the excitation energy of atom is lower than the ionization energies of atom, the photons from excitation radiation of molecules have not energies enough to take off electrons from O_2 molecules according to the atomic physics and the quantum mechanism.

For another radiation, the recombination of electron and positive oxygen ion may release photons and the energy of released photons is

$$h\nu_m = eU_i + E_k, \tag{1}$$

where ν_m is the frequency of photon from recombination radiation, eU_i is the ionization energy of O_2 molecule and E_k is the kinetic energy of electrons participating in recombination reaction.

The reacting process of recombination are given by

$$O_2^+ + e = O_2 + h\nu_m. \tag{2}$$
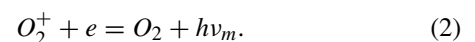
The above (1) obviously discovers the energy of released photons is greater than or equal to the ionization energy. This implies that a photon only from recombination radiation has the energy enough to be capable to impact off an electron out of an O_2 molecule.

In contrast to the excitation radiation of O_2 molecules, it is easily found that only the recombination radiation is capable to ionize electrons from neutral O_2 molecules. Especially, due to the restrictions of the quantum mechanism, namely the fact that the probability of two energy level transitions of electrons in oxygen molecules is so small as to be negligible,

the electrons cannot be ionized from O_2 molecules by the continuous excitation radiation.

Besides, because of a direct correspondence between the frequency and energy of photon, the photon frequency is derived as

$$\nu_m = \frac{eU_i + E_k}{h} \geq \frac{eU_i}{h} \qquad (3)$$

The above equation indicates that due to the fact that the moving electrons have the different kinetic energies the photons released by recombination can own diverse frequencies whose the minimum value $\nu_{min} = \frac{eU_i}{h}$. Particularly, this equation directly discovers that different kinetic energies of electrons correspond to different frequencies of photons of recombination radiation.

Noticeably, according to the correspondence between photonic frequency and photonic energy the frequency of photon emitted by the meta-stable molecules turning back to the ground molecules is less than or equal to that of photon with the ionization energy of oxygen molecules, which may give the relation

$$\nu_m \geq \nu_{min} > \nu_{exc} \qquad (4)$$

where ν_{exc} is the frequency of photon from excitation radiation of molecule.

The above inequality precisely reveals that the photon with the frequency larger than the minimum value $\frac{eU_i}{h}$ is qualified to cause discharging while the photon with the energy less than eU_i is not granted. In the study of Akishev *et al.* [15], it is also reflected that only the high frequency radiation (namely the high energy photon) is responsible for the photo-ionization of pure gas.

These analyses demonstrate that only the photons produced by recombination of e and O_2^+ may ionize O_2 to generate the new seed electrons but the photons released by the energy level transition of meta-stable O_2^* turning back to the ground state O_2 cannot ionize new seed electrons. Thus we call the photons from recombination of e and O_2^+ as effective photons during the process of discharge. However, in some previous documents the inaccurate concept is even presented, which is that neutral molecules encountered in the path of the photon radiation from the excitation of molecules may be ionized, releasing the seed electrons in pure gas.

By the above discussions, the moving electrons joining the recombination reaction in the electric field carry various kinetic energies. Moreover the kinetic energies of electrons and the binding energy released by recombination are converted to the energies of photons of recombination radiation. This implies the photons generated from recombination may hold diverse frequencies. In the meantime, these photons may ionize the seed electrons from oxygen molecules. Based on the conservation of energy, the kinetic energy E_k^{seed} of seed electron which from O_2 molecule is ionized by a photon is given by

$$E_k^{seed} = h\nu_m - eU_i \qquad (5)$$

This equation implies that the photon of energy higher than the ionization energy can produce the seed electron and also signifies that the photons with diverse frequencies can generate the seed electrons with different kinetic energies. These seed electrons with diverse energies trigger the different electron avalanches, which suggests the chaotic discharge behaviors may occur in the positive corona. However, until now the relevant studies haven't still given a clear explanation on the chaotic discharging phenomenon of positive corona.

We have a conclusion: the photons from recombination of e and O_2^+, which have diverse radiation frequencies, may result in the different electron avalanches triggering discharging; especially, the photons with diversified frequencies are a key factor leading to the chaotic discharging phenomenon of positive corona.

B. MICROSCOPIC PHYSICAL MODEL

The positive current density j_i and the electron current density j_e are proportional to the electric field E and the positive ion density n_i or the electron density n_e respectively, which are given by

$$j_i^+ = \mu_i n_i E \qquad (6)$$

and

$$j_e = \mu_e n_e E \qquad (7)$$

where μ_i and μ_e are the corresponding mobility of positive ion and electron.

The photo-ionization process plays an indispensable role in the sustaining electron avalanche of positive corona discharge. The photo-ionization is usually assumed to be the vital mechanism for the production of seed electrons causing the propagation of electron avalanches.

The high frequency photons produced by the recombination of electrons and oxygen positive ions decide the photo-ionization whether to occur, as is mentioned in the analysis of the above section. For simplicity, all of high frequency photons are supposed to photo-ionize oxygen molecules generating seed electrons. Thus, the recombination reaction may measure the photo-ionization reaction and meanwhile the recombination parameter may be used to represent the degree of photo-ionization. Especially, the recombination reaction generating the high frequency photons can be treated as a source producing seed electrons prepared for the next avalanche.

Meanwhile, some electrons kn_e impact-excite O_2 into meta-stable O_2^* and then attach to O_2 transforming into O_2^- negative ions; meta-stable O_2^* radiate photons γ, turning back into O_2. The process may be expressed as the reactions below

$$O_2 + e = O_2^* + e \qquad (8)$$
$$O_2^* = O_2 + \gamma \qquad (9)$$
$$O_2 + e = O_2^-. \qquad (10)$$

Adding three above reactions, by simplifying the brief relation is derived as

$$O_2 + e = O_2^- + \gamma$$

Strictly speaking, the attachment, impact-ionization, excitation and photo-ionization in the process of positive corona discharge are of non-locality, which means that these reactions can occur synchronously at any same point in the ionization layer.

Seeing that the kinetic energy of electrons kn_e is lowered through e-O_2 impact-excitation, each one of these electrons may be assumed to attach to a ground state O_2 molecule. The number density of negative ions is then

$$n_i^- = kn_e \qquad (11)$$

where k is the attachment parameter of O_2 molecule. These electrons kn_e are consumed for attaching to O_2 and then don't participate in the propagated electronic current density. The negative ions O_2^- form the negative ion current density j_i^- which is obtained as

$$j_i^- = \mu_i n_i^- E = \mu_i kn_e E \qquad (12)$$

where negative ions have the mobility same to the mobility μ_i of positive ion due to the negligible mass of attached electrons. The negative ions O_2^- are also regarded as another source producing seed electrons to reserve electrons for the next avalanche.

Additionally, since a few moving electrons ϑn_e are used for recombination with O_2^+, these electrons ϑn_e are removed from total moving electrons.

Accordingly the effective electron current density is thus defined as

$$j_e' = (n_e - \vartheta n_e - kn_e)\,\mu_e E \qquad (13)$$

where ϑ is the recombination parameter of O_2^+ and e.

This formula discovers the physical correlation among the seed electron, photo-ionization and the attachment, and builds a clear and profound mathematical expression while the relevant description on photo-ionization in the previous documents is complicated and based on the empirical formula.

According to (6), (12) and (13), the total electrical current density is expressed as

$$j_{total} = j_i^+ + j_i^- + j_e' = \mu_i n_i E + k\mu_i n_e E$$
$$+ (n_e - \vartheta n_e - kn_e)\,\mu_e E \qquad (14)$$

Then the internal electric current, which is resulting from the moving charged particles in the discharge layer, is given:

$$I = eS\,[\mu_i n_i E + k\mu_i n_e E + (n_e - \vartheta n_e - kn_e)\,\mu_e E] \qquad (15)$$

where S is the spherical surface area around anode and e is the unit Coulomb charge.

Considering that the position of discharge is near electrode, the space charge is approximate to the surface charge Q on the anode at the beginning of discharging. According to the conservation law of charge, the continuity equations of charge Q with time t is

$$\frac{dQ}{dt} = \frac{V_c}{R} - \frac{Q}{\tau} - I \qquad (16)$$

where R is the exterior equivalent resistance of discharge system and V_c is the corona applied voltage of electrode.

The strength of electric field close to the discharge electrode is

$$E = \frac{Q}{\varepsilon_0 S} \qquad (17)$$

where ε_0 is the permittivity of vacuum.

The effective electric capacity of spherical inner electrode is shown as following

$$C = 4\pi\varepsilon_0 r \qquad (18)$$

where r is the distance to the center of anode.

The applied voltage V_c of discharge system is expressed as

$$V_c = \frac{\varepsilon_0 E_c S}{C} \qquad (19)$$

and the surface charge Q is

$$Q = \varepsilon_0 E S \qquad (20)$$

The initial strength of field near the surface of anode is

$$E_c = \frac{V_c C}{\varepsilon_0 S} = \frac{V_0 4\pi\varepsilon_0 r_a}{\varepsilon_0 4\pi r_a^2} = \frac{V_c}{r_a} \qquad (21)$$

where r_a is the radius of inner electrode.

At the beginning of discharge, the initial strength of electric field in the discharge layer can be expressed as

$$E_r = \frac{V_c C}{\varepsilon_0 S} = \left(\frac{r_a}{r}\right)^2 \frac{V_0}{r_a} = \left(\frac{r_a}{r}\right)^2 E_c \qquad (22)$$

with

$$\left(\frac{r_a}{r}\right)^2 \leq 1 \qquad (23)$$

Substituting (15), (17), (19) and (22) into (16), the equation with the explicit electric field strength E is obtained as

$$\frac{\partial E}{\partial t} = \left(\frac{r_a}{r}\right)^2 \frac{E_c}{\tau} - \frac{E}{\tau} - \frac{e}{\varepsilon_0} E[\mu_i n_i + k\mu_i n_e +$$
$$+ (n_e - \vartheta n_e - kn_e)\,\mu_e] \qquad (24)$$

where $\tau = RC$ is the characteristic time of positive corona discharge system and it may be obtained by the experimental measures.

To simplify the question, we research on the discharge near the surface of anode and thus take the value of $\left(\frac{r_a}{r}\right)^2$ which approximates to 1, namely

$$\left(\frac{r_a}{r}\right)^2 \sim 1 \qquad (25)$$

Then, equation (24) can be

$$\frac{\partial E}{\partial t} = \frac{E_c}{\tau} - \frac{E}{\tau} - \frac{e}{\varepsilon_0} E[\mu_i n_i + k\mu_i n_e$$
$$+ (n_e - \vartheta n_e - kn_e)\,\mu_e] \qquad (26)$$

Notably, this equation incorporates the recombination, attachment and photo-ionization, which significantly reduces the complexity of discharge system.

In the meantime, the continuity equation of charged particles is written as,

$$\frac{\partial n}{\partial t} = -\nabla \cdot j + \alpha j \tag{27}$$

where n is the number density of charged particles, j is the corresponding current density and α is Townsend's first ionization coefficient.

Besides, Townsend's first ionization coefficient on impact-ionization near the anode may linearly approximate to

$$\alpha = AP(\frac{E}{E_0} - 1) \tag{28}$$

with

$$E_0 = \frac{W_i}{el_0} \tag{29}$$

where E_0 is the critical electric field strength, W_i is the ionization energy of oxygen molecule, A is the characteristic parameter of gas, l_0 is the average free path of electron and P is the gas pressure.

C. DYNAMICAL EQUATIONS

In our theory, the electric field equation incorporates the recombination, attachment and photo-ionization processes. In the meantime, the continuity equations for the electric field, electrons and positive ions are detailedly expressed. These three equations constitute the governing equations. Compared with the results of previous theory [14], [15], [25], our method simplifies the complexity of discharge system to easily identify problem spots. For a spherically symmetrical coordinate system, the governing equations are given by

$$\frac{\partial E}{\partial t} = \frac{E_c}{\tau} - \frac{E}{\tau}$$
$$- \frac{e}{\varepsilon_0} E[\mu_i n_i + k\mu_i n_e + (n_e - \vartheta n_e - kn_e)\mu_e] \tag{30}$$

$$\frac{\partial n_e}{\partial t} = AP\left(\frac{E}{E_0} - 1\right)\mu_e n_e E$$
$$- \mu_e E \frac{1}{r^2}\frac{\partial r^2 n_e}{\partial r} - \frac{e}{\varepsilon_0}\mu_e n_e n_i + \frac{e}{\varepsilon_0}\mu_e n_e^2 \tag{31}$$

$$\frac{\partial n_i}{\partial t} = AP\left(\frac{E}{E_0} - 1\right)\mu_e n_e E$$
$$- \mu_i E \frac{1}{r^2}\frac{\partial r^2 n_i}{\partial r} + \frac{e}{\varepsilon_0}\mu_i n_e n_i - \frac{e}{\varepsilon_0}\mu_i n_i^2 \tag{32}$$

Due to the fact that comparing with the particles' motion caused by the electric field the diffusion motion of particles is relatively very small, the diffusion effect of electrons and ions can be neglected in the discharge in order to clearly describe the main characteristics of oscillation discharge. Simultaneously, the main factors of discharge process including the excitation, ionization, photo-ionization, recombination of electrons with positive ions and attachment of electrons to

neutral molecules, are considered in our dynamical equations although the above governing equations apparently seem brief.

We select the physical quantities n_e, n_i and E as explicit variables is because n_e, n_i and E firstly participate in the primary ionization reaction in an electron avalanche while photons, negative ions and meta-stable oxygen molecules are produced from the primary ionization reaction and the secondary reaction. This point accounts for that other physical quantities may be dominated by n_e, n_i and E. Moreover, we also can significantly decrease the number of equations and the number of variables. Thus we may profoundly investigate the dynamical mechanism and discharge characteristics of positive corona discharge with time.

D. NONLINEAR COUPLED OSCILLATOR

The chaotic discharging phenomenon in the positive corona is rarely discussed in previous literatures. Due to the complexity of chaotic discharge of positive corona, the chaotic discharge was avoided in lots of researches. The previous theoretical studies on positive corona discharge merely give the discharging pattern of periodic pulses and stationary-state. However, the actual positive corona system displays the chaotic pulsed output during the process of discharge [2]. This reflects the early models are insufficient to describe the actual discharge of positive corona. Thus it is needed to figure out the intrinsic mechanism of positive corona discharge and establish a dynamical model to more accurately discover the actual discharge of positive corona.

According to our analysis on photo-ionization producing seed electrons, we find that the electrons photo-ionized by photons with a certain frequency from recombination radiation can trigger a Trichel pulsed output with the correspondingly certain period, namely that the photons with a certain frequency can lead to a correspondingly periodic discharge. Additionally due to the different kinetic energy of moving electrons recombined with positive ion, the frequencies of recombination radiation are various, as mentioned above in the discussion of section II.A. Then the diversified photons with different frequencies may give rise to the correspondingly diversely periodic pulsed-discharge constituents. Based on the above analysis, in the actual positive corona system the total discharge output should be coupled by multi-different periodic discharge constituents. This is the reason observing the aperiodic Trichel pulsed discharge, i.e. the chaotic Trichel pulsed output.

In the meantime, it is known that the different frequency photon has the correspondingly different ionization rate. Meanwhile, considering that the energies of recombination photons are higher than the ionization energy of oxygen molecules, for simplicity it is assumed that all recombination photons ionize O_2 molecules. This means that the different recombination parameters ϑ can correspond to the types of recombination photons with the different frequency. Moreover, the photons with certain frequency ionize the electrons out of O_2 molecules as seed electrons and meanwhile these

seed electrons with certain initial energy trigger the electron avalanche with a certain pattern. This indicates that for our nonlinear system when the recombination parameter ϑ takes a determined value the governing equations may have a certain periodic output mode. Then, the different recombination parameters can mean the distinct frequency output modes of discharge.

According to the above discussion on the physical mechanism of chaotic discharge, our nonlinear system may be treated as the complex discharge system coupled by multi-single systems, which is called the coupled oscillator [26]–[29]. To conveniently describe and easily demonstrate the aperiodic discharge phenomena of positive corona, we select two single nonlinear oscillators [26]–[29] with different recombination parameters ϑ to construct a nonlinear coupled complex system while the attachment parameter k takes a fixed value. Therefore, the high-dimensional nonlinear complex oscillator is given as follows:

$$\frac{\partial E^1}{\partial t} = \frac{E_c}{\tau} - \frac{E^1}{\tau} - \frac{e}{\varepsilon_0}E^1[\mu_i n_e^1 + k\mu_i n_e^1 \\ + \left(n_e^1 - \vartheta_1 n_e^1 - kn_e^1\right)\mu_e] \tag{33}$$

$$\frac{\partial n_e^1}{\partial t} = AP\left(\frac{E^1}{E_0} - 1\right)\mu_e n_e^1 E^1 - \mu_e E^1 \frac{1}{r^2}\frac{\partial r^2 n_e^1}{\partial r} \\ - \frac{e}{\varepsilon_0}\mu_e n_i^1 n_e^1 + \frac{e}{\varepsilon_0}\mu_e n_e^{1^2} \tag{34}$$

$$\frac{\partial n_i^1}{\partial t} = AP\left(\frac{E^1}{E_0} - 1\right)\mu_e n_e^1 E^1 - \mu_i E^1 \frac{1}{r^2}\frac{\partial r^2 n_i^1}{\partial r} \\ + \frac{e}{\varepsilon_0}\mu_i n_e^1 n_i^1 - \frac{e}{\varepsilon_0}\mu_i n_i^{1^2} \tag{35}$$

$$\frac{\partial E^2}{\partial t} = \frac{E_c}{\tau} - \frac{E^2}{\tau} - \frac{e}{\varepsilon_0}E^2[\mu_i n_e^2 + k\mu_i n_e^2 \\ + \left(n_e^2 - \vartheta_2 n_e^2 - kn_e^2\right)\mu_e] \tag{36}$$

$$\frac{\partial n_e^2}{\partial t} = AP\left(\frac{E^2}{E_0} - 1\right)\mu_e n_e^2 E^2 - \mu_e E^2 \frac{1}{r^2}\frac{\partial r^2 n_e^2}{\partial r} \\ - \frac{e}{\varepsilon_0}\mu_e n_i^2 n_e^2 + \frac{e}{\varepsilon_0}\mu_e n_e^{2^2} \tag{37}$$

$$\frac{\partial n_i^2}{\partial t} = AP\left(\frac{E^2}{E_0} - 1\right)\mu_e n_e^2 E^2 - \mu_i E^2 \frac{1}{r^2}\frac{\partial r^2 n_i^2}{\partial r} \\ + \frac{e}{\varepsilon_0}\mu_i n_e^2 n_i^2 - \frac{e}{\varepsilon_0}\mu_i n_i^{2^2} \tag{38}$$

$$n_e = 0.5n_e^1 + 0.5n_e^2 \tag{39}$$

$$n_i = 0.5n_i^1 + 0.5n_i^2 \tag{40}$$

$$E = 0.5E^1 + 0.5E^2 \tag{41}$$

$$j_{total} = 0.5j_{total}^1 + 0.5j_{total}^2 \tag{42}$$

where for the complex discharge system, the total electron number density n_e is separated to n_e^1 and n_e^2, the total positive number n_i is separated to n_i^1 and n_i^2 and the surface electric field E is separated to E^1 and E^2. n_e^1, n_i^1, E^1 and n_e^2, n_i^2, E^2 are the variables of single system1 and single system 2, respectively. Additionally, E_c is used as the control parameter

of discharge system. For simplicity, it is assumed that each output component for single system has the same proportion to total output. Thus, the weight factor of each single system to the nonlinear complex system is set to 0.5.

E. NUMERICAL IMPLEMENTATION AND PARAMETERS SETTING

To better analyze the phenomena and natures of positive corona discharge, in present calculations the dimensionless parameters of equations are adopted. The applied voltage $V = \mathbf{V}/V_0$, where $\mathbf{V}$ and V_0 are the actual voltage and the critical discharge voltage respectively; the surface electric field strength $E = \mathbf{E}/E_0$, where E_0 is the critical electric field strength and $\mathbf{E}$ is the actual surface electric field strength; $n_e = \mathbf{n_e}/n_0$, $n_i^+ = \mathbf{n_i^+}/n_0$ and $n_i^- = \mathbf{n_i^-}/n_0$, where n_0 is the number density of air at a standard atmospheric pressure and meanwhile $\mathbf{n_e}$, $\mathbf{n_i^+}$ and $\mathbf{n_i^-}$ are the actual number densities respectively; additionally, the time of evolution $t = \mathbf{t}/\boldsymbol{\tau}$, where $\tau = \boldsymbol{\tau}$, $\boldsymbol{\tau}$ is the characteristic time of positive corona system and $\mathbf{t}$ is the actual evolutionary time.

In this research, the critical discharge voltage V_0 is set to $12.5kV$, the radius of discharge electrode r_a is set to 1mm, the equivalent exterior resistance R is set to $3k\Omega$, the number density of air is given by $2.69 \times 10^{25}\mathrm{m}^{-3}$ and the average free path l_0 of electron is set to 1×10^{-6}m at a standard atmospheric pressure; the ionization energy and the excitation energy of oxygen molecule are 12.50eV and 7.90eV respectively; the electron mobility $\mu_e = 2 \times 10^{-2}\mathrm{m}^2\mathrm{V}^{-1}\mathrm{s}^{-1}$ and the ion mobility $\mu_i = 2 \times 10^{-4}\mathrm{m}^2\mathrm{V}^{-1}\mathrm{s}^{-1}$. In the meantime, the attachment parameter k is set to 0.6 and the recombination parameters ϑ are set to 0.17 and 0.28. Additionally, the discharge gas is pure O_2 at a standard atmospheric pressures and room temperature; and the calculation is carried out based on Mathematica 12.

In our research, seeing that there are many previous investigations on spatial characteristics of positive corona discharge, we focus on the variations of discharge outputs with time and the dynamic natures of positive corona discharge. On the basis of the spatial distribution of discharged particles in the previous studies, the spatial items of equations near the surface of anode may take the appropriate values as reference values. Then, we rationally diminish the complexity of equations and meanwhile are better concerned with the questions of the time evolutions of positive corona discharge and the dynamic discharge behaviors.

III. PHYSICAL PROCESS AND DYNAMIC MODEL
A. NONLINEAR PROCESS DISCUSSION
The analysis of nonlinear time series and trajectory phase portraits is an effective method for the study on complicated dynamical phenomena [30], [31], which can reveal importantly intrinsic characteristics of nonlinear system. Hence it is necessary to investigate the dynamic mechanism of positive corona discharge through nonlinear time series analysis and trajectory phase portraits.
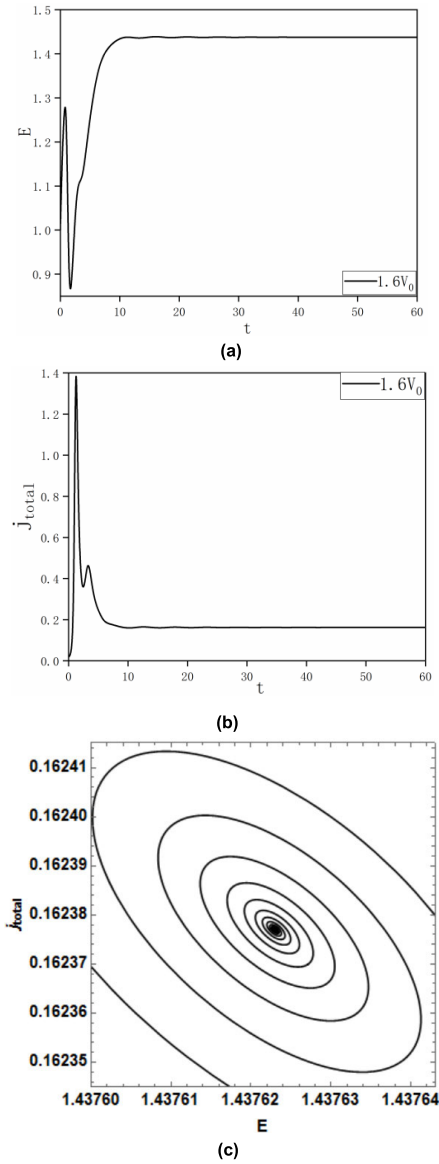
(a)

(b)

(c)

FIGURE 3. (a). The time series of surface electric field strength E for 1.6V_0: over-damped behaviour of nonlinear oscillator. (b). The time series of total current density j_{total} for 1.6V_0: over-damped behavior of nonlinear oscillator. (c). The simple attractor of corona system namely: the stable fixed point with spiral trajectories in 2D phase portraits.

(a)

(b)

(c)

FIGURE 4. (a). The time series of surface electric field strength E for 2.1V_0: the damped behavior of nonlinear oscillator. (b). The time series of total current density j_{total} for 2.1V_0: the damped behavior of nonlinear oscillator. (c). The simple attractor of corona system namely: the stable fixed point with spiral dense trajectories in 2D phase portraits.

In this section, different stages of discharging are displayed. With the applied voltage increasing, the nonlinear system on the positive corona discharge gradually produces the point attractor, limit cycle and strange attractor [26]–[29].

At the beginning of discharge, when the applied voltage sets to 1.6V_0, the system discharging has the nonzero-stationary state outputs of electric field and total current density after experiencing an initial transient stage. These two time series are plotted in Fig. 3(a) and 3(b).

In the two-dimensional phase shown in Fig. 3(c), all trajectories spiral into the stable fixed point, which means the outputs of electric field and current density gradually become steady values.
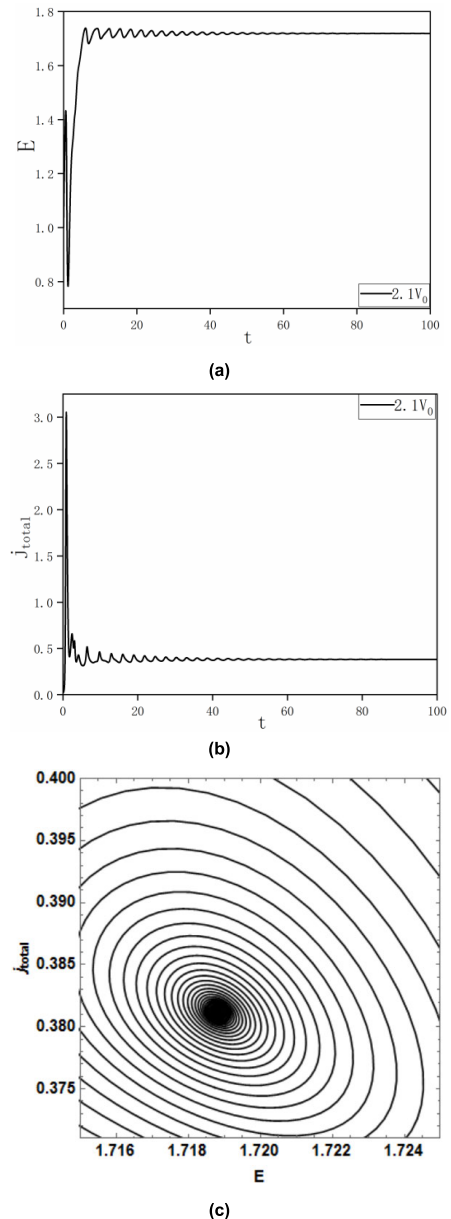
As shown in Fig. 4(a) and 4(b), when the onset voltage rises up to 2.1V_0, with time the electric field E and the total electric current density j_{total} display a damped waveform and gradually decay to a constant output after the initial stage of drastic oscillation.

Fig. 4(c) depicts all trajectories asymptotically spiral inwards towards a stable fixed point which is called a point attractor, manifesting the electric field and current density gradually reach steady values of outputs after experiencing unstable outputs. Moreover, this phase graph has more dense trajectories than that of 1.6V_0.
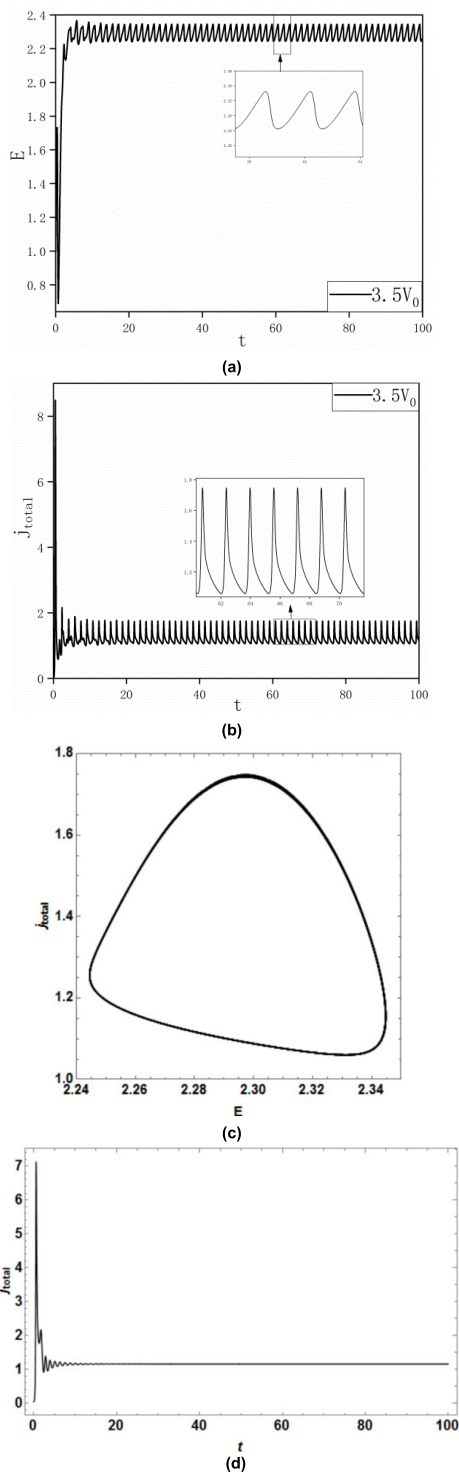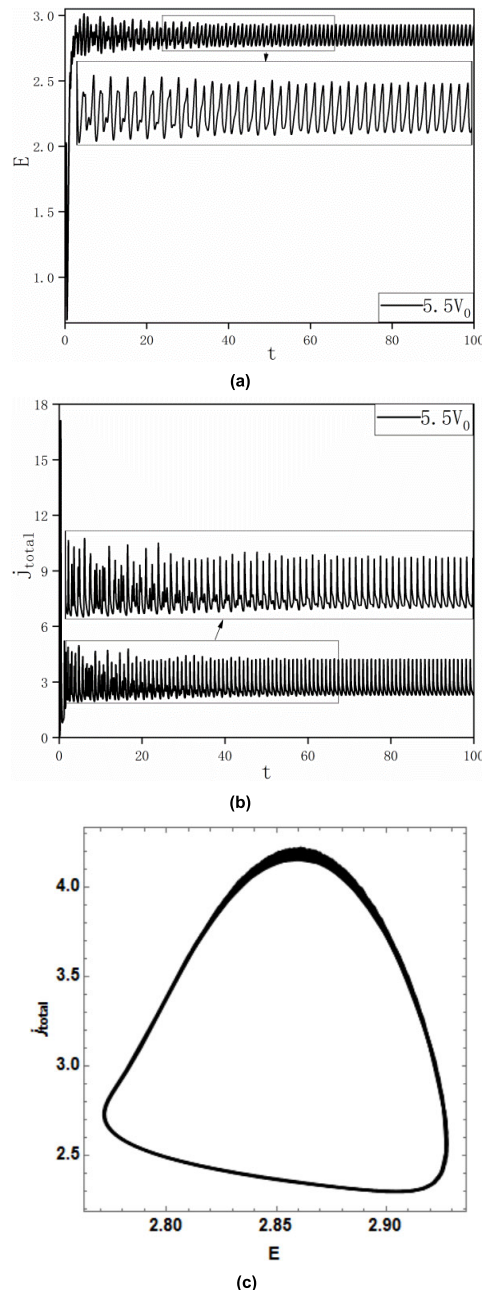
(a)

(b)

(c)

(d)

FIGURE 5. (a). The time series of surface electric field strength E with the zoomed in view for 3.5 V_0: the periodic behaviour of nonlinear oscillator. (b). The time series of total current density j_{total} with the zoomed in view for 3.5 V_0: the periodic behavior of nonlinear oscillator. (c). The periodic attractor of corona system the stable limit circle in 2D phase portraits for 3.5 V_0. (d). The time series of total current density j_{total} for 3.5 V_0 at the recombination parameter $\vartheta = 0$.

As is seen in Fig. 5(a) and 5(b), for $V = 3.5V_0$ the outputs of positive corona settle into a periodic oscillation with time after a initial transient; for clear observation, the

(a)

(b)

(c)

FIGURE 6. (a). The time series of surface electric field strength E for 5.5V_0: the damped behaviour of nonlinear oscillator in transition to quasi-periodic fluctuation. (b). The time series of total current density j_{total} for 5.5V_0: the damped behavior of nonlinear oscillator in transition to quasi-periodic fluctuation. (c). The quasi-periodic attractor of corona system: the quasi-periodic orbit in 2D phase portraits for5.5 V_0.

zoomed in segments of two small squares in Fig. 5(a) and 5(b) reflect a typically periodic wave with sharp-jagged shapes. Especially, the varying pattern of total current density and the characteristic of pulse are consistent with the previous researches [3], [4], [12].

The two-dimensional phase portrait in Fig. 5(c) shows a typical periodic orbit, meaning at $V = 3.5V_0$ the attractor is a simple stable limit cycle. This also signifies the outputs of electric field and current density repeat with a fixed period.

As observed in Fig. 5(d), when the recombination parameter $\vartheta = 0$, the output of the total electric current density j_{total} settles to a constant output after experiencing a damped oscillation and cannot stay a regularly periodic oscillation analogous to the periodic waveform shown in Fig. 5(b).

For $V = 5.5V_0$, as seen in Fig. 6(a) and 6(b), there is a transient chaos about the outputs of E and j_{total} with $t < 80t_0$ and then the system approaches to periodically oscillate with higher frequency than that for the prior 3.5 V_0. To make this process clearer, the enlarged segments are depicted, showing the obvious transition from the irregular jagged waves to the regularly periodic pulses. In the meantime, the maxima in successive E and successive j_{total} are no longer equal; the neighboring peaks become a little higher or a little lower than the typically periodic trains, as seen in Fig. 6(a) and 6(b). These mean with the applied voltage increasing the periodic outputs of discharge start becoming unstable.

Fig. 6(c) shows the trajectories in 2D phase diagram slightly deviate from the initial orbit. There is a quasi-periodic orbit although it is a stable limit cycle, which further illustrates the pulses of outputs become slightly irregular and don't simply repeat in the two respective time-series of E and j_{total}.

According to the analysis on the time series and 2D trajectories, the discharge system has the quasi-steady outputs at $5.5V_0$.

When the onset voltage remains rising to $6.6V_0$, the aperiodic appearance of outputs suggests the positive corona discharge begins having slightly chaotic oscillations, as shown in Fig. 7(a) and 7(b). For clearer observation, as seen in the enlargement of small squares, the spike-shape of pulses is obviously deformed and irregular, accounting for with the increase of applied voltage the periodic characteristic of corona discharge becomes comparatively weaker but the irregular characteristic becomes stronger.

2D and 3D phase space in Fig. 7(c) and 7(d) display 'aperiodic long-term behavior', which means that the trajectories do not settle down to a fixed point, or periodic or quasi-periodic orbit. Additionally in 2D and 3D phase diagram, it is visibly found that the closed orbits of phase portraits show a fractal structure and self-similarity, the pattern of which reflects that there is no longer a periodic orbit and all trajectories spiral towards the strange attractor. Especially, compared with the phase portraits of periodic outputs the orbits in Fig 7(c) and 7(d) are twisted and stretched. These indicate the occurrence of slightly chaotic attractor in phase space and reveal the aperiodic dynamic characteristics of the positive corona discharge.

As shown in Fig. 8(a) and 8(b), after an initial transient process, the outputs of E and j_{total} settle into an irregular oscillation that persists as $t \to \infty$, but never repeats exactly. The time series are aperiodic fluctuations. Obviously, a typically chaotic output occurs at $8V_0$.
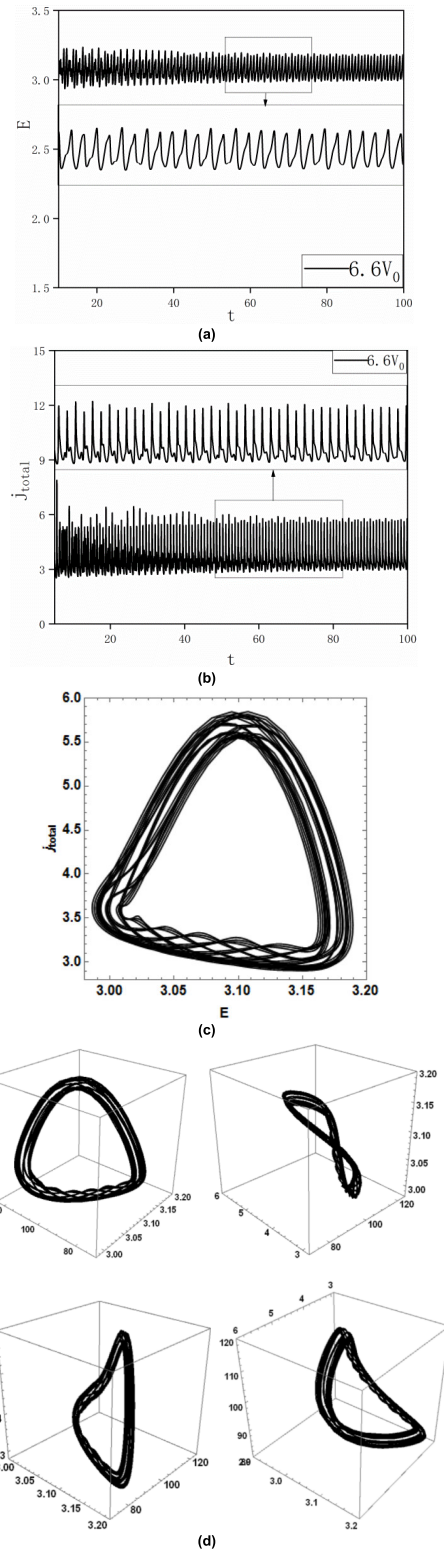

FIGURE 7. (a). The time series of surface electric field strength E with the zoomed in view for $6.6V_0$: the aperiodic behaviour of nonlinear oscillator with slightly irregular oscillation. (b). The time series of total current density j_{total} with the zoomed in view for $6.6V_0$: the aperiodic behavior of nonlinear oscillator with slightly irregular oscillation. (c). The strange attractor of corona system in 2D phase portraits for 6.6 V_0: the self-similarity and aperiodic orbits.
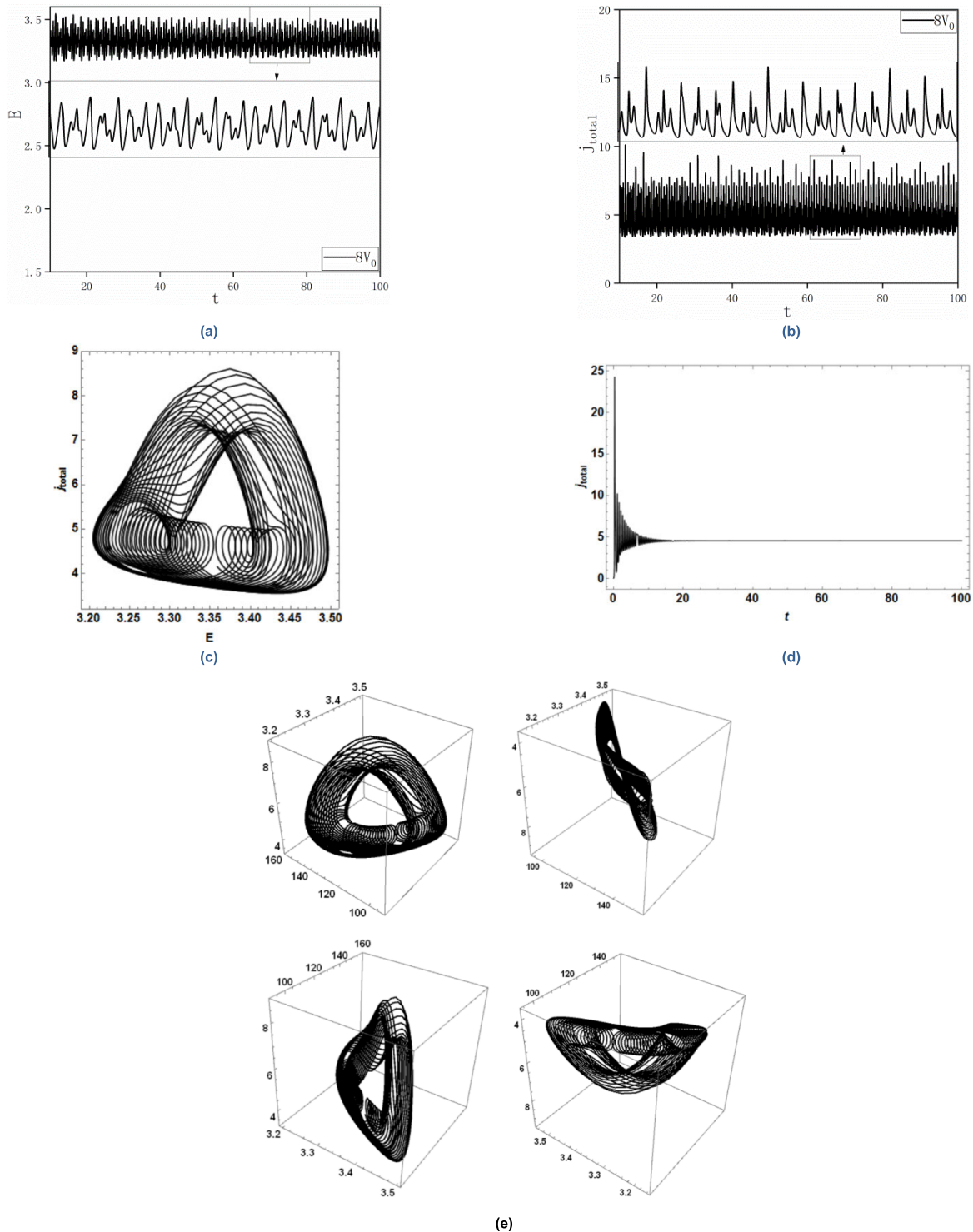
FIGURE 8. (a). The time series of surface electric field strength E: with the zoomed in view for $8V_0$: the aperiodic behavior of nonlinear oscillator with irregular fluctuation. (b). The time series of total current density j_{total} with the zoomed in view for $8V_0$: the aperiodic behavior of nonlinear oscillator with irregular fluctuation. (c). The strange attractor of corona system in 2D phase portraits for $8\,V_0$: the self-similarity and aperiodic orbits. (d). The time series of total current density j_{total} for $8\,V_0$ at the recombination parameter $\vartheta = 0$. (e). The strange attractor on j_{total}-E-n_i^+ in 3D phase space for $8V_0$: the self-similarity and aperiodic orbits.

Zooming into both E-t and j_{total}-t series exhibits attractive ragged-spike pulses, illustrating although the recurrent characteristic of time series is revealed by the fact that the certain pattern of the waveform repeats itself at irregular intervals, there never exists the precise repetition and circulation and the oscillation is surely aperiodic.

The phase portraits of 2D and 3D in Fig.8(c) and 8(e) clearly exhibit the characteristics of fractal and similarity of orbits, which is a typical strange attractor. Meanwhile, as is seen from the phase portraits, the dynamic orbits of this strange attractor show obviously folding and twisting. These signify that with further rise of applied voltage, the chaotic nature of discharge system is more prominent.

As seen in Fig. 8(d), compared with the case at $3.5V_0$, although the applied voltage rises to $8V_0$, at the recombination parameter $\vartheta = 0$ the total electric current density j_{total} still displays a damped oscillation rapidly decaying to a constant output, rather than decaying to an irregular waveform (similar to the irregular oscillation shown in Fig.8(b)) after the initial transient stage of drastic oscillation.

Fig. 9(a) and 9(b) show the outputs of E and j_{total} settle into an irregular oscillation. Moreover, zooming in the pictures, the ragged-spike pulses of E-t and j_{total}-t series can be clearly observed. Apparently a certain inherent structure of recurrent characteristic of irregular intervals is seen in the waveform of time series. However, the time series never have a real periodicity and exact repetition. These points discover there is the chaotic discharge phenomenon at $10V_0$ onset voltage.

For the applied voltage $10V_0$, in the 2D and 3D phase space shown in Fig. 9(c) and 9(d), in contrast with the case at $8V_0$ this strange attractor has conspicuous self-similarity and an internal recurrent structure which is analogous to a layered-structure. This is a typical fractal of chaos. Due to further stretching and folding, the chaotic attractor is deformed significantly and very different from that of $8V_0$. This indicates that within a certain high applied voltage range the positive corona discharge system in our research may generate irregularly chaotic outputs.

Noticeably, this nonlinear complex system is deterministic because there is no random input or parameters. Simultaneously, according to the above analyses the nonlinear complex system has chaotic behaviors because under high applied voltage the trajectories do not settle down to a fixed point, or periodic or quasi-periodic orbit. The system is also called as the nonlinear coupled oscillator.

Especially, for the time-series outputs, 2D and 3D phase portraits of electric field E and total electric current density j_{total}, it is revealed that the applied voltage as a control parameter decides the different output patterns of positive corona discharge. This is the first time that a nonlinear dynamic model is proposed to predict the chaotic discharging phenomenon on the positive corona based on the microscopic level of intrinsic physical mechanism.

By the investigation of the nonlinear discharge, we preliminarily find out a dynamical mechanism: a nonlinear complex system can be coupled by nonlinear single systems; furthermore, at least two pure periodic systems may be coupled into a chaotic system. Correspondingly, as for producing the chaotic discharge, the microscopic physical mechanism at
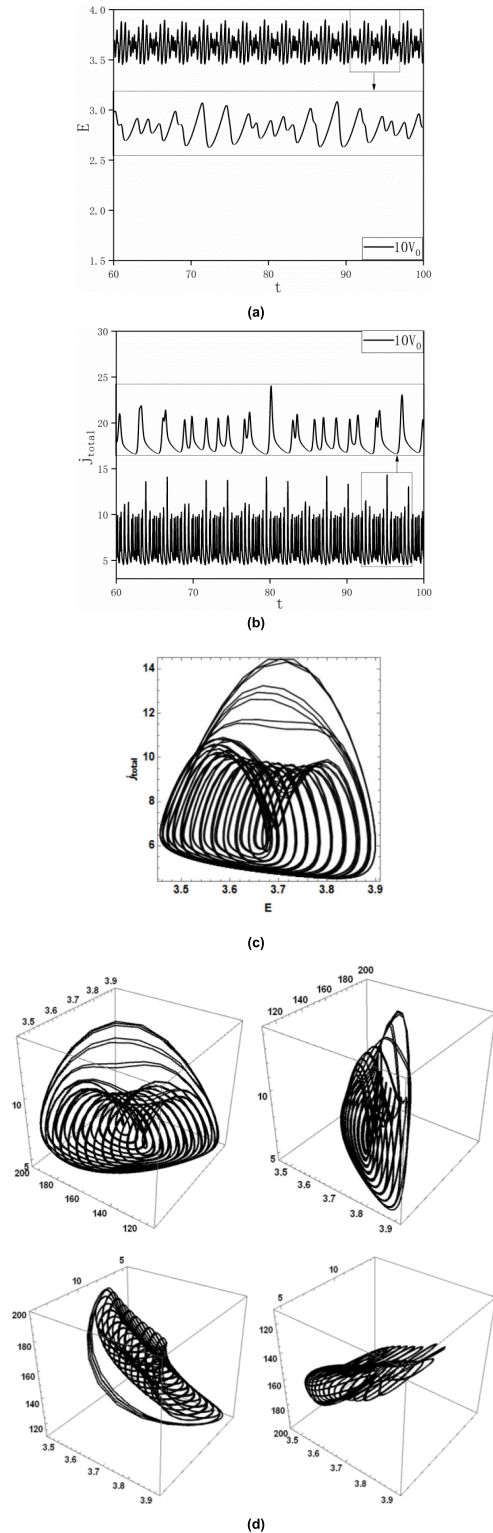

FIGURE 9. (a). The time series of surface electric field strength E with the zoomed in view for $10V_0$: the aperiodic behavior nonlinear oscillator with irregular fluctuation. (b). The time series of total current density j_{total} with the zoomed in view for $10V_0$: the aperiodic of behavior of nonlinear oscillator with irregular fluctuation. (c). The strange attractor of corona system in 2D phase portraits for 10 V_0: the self-similarity and aperiodic orbits. (d). The strange attractor on j_{total}-E-n_i^+ in 3D phase space for $10V_0$: the self-similarity and aperiodic orbits.

a molecular or atomic level is further discovered: namely since the high-energetic photons with diverse frequencies may give rise to the discharge output components of different periods, for the system of positive glow corona discharge the total chaotic discharge output can be understood to be coupled by the various periodic-discharge components.

For profound dynamical analysis, our nonlinear complex system can realize that a constant external excitation rather than a varying or periodic external excitation (namely for positive corona discharge, the constant applied voltage rather than the varying or periodic applied voltage) causes a non-steady state output, such as a periodic or chaotic oscillation output. Furthermore, we independently find that the photons occurring can be mathematically treated as the feedback signal. This feedback mechanism plays a major part in the pulsed discharge including a regular or irregular form. Especially, due to the feedback the system can produce a non-stationary state output under a constant external excitation. In other word, if the recombination term is canceled, namely that no photo-ionization appears, then there exist no continuous pulses during discharge, as seen in Fig.5(d) and Fig.8(d), although the applied voltages rise. Speaking from the micro level, the photons occurring as the feedback mechanism is prepared for the next electron avalanche, namely for the next pulse discharge.

In contrast with previous researches, our dynamical model realizes the chaotic discharge of positive glow corona, which is the highlight of our work. Although the chaotic discharge of positive corona is observed in many experimental studies, so far there was no a good theoretical model proposed to predict and explain the chaotic discharge of positive corona before our study.

B. ANALYSIS AND DISCUSSION OF POSITIVE CORONA DISCHARGE

This section is concerned with the characteristics of average current density and pulsed frequency vs. applied voltage and the discharge behaviors of diverse current densities and various particles.
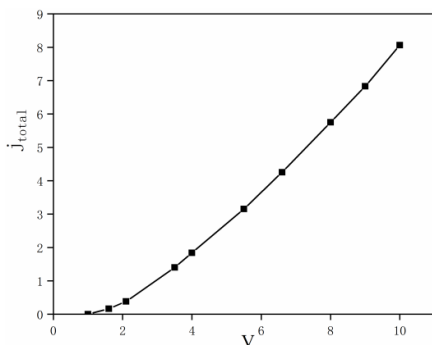
FIGURE 10. V-I characteristic curve for average current density vs. applied voltage.

1) I-V CHARACTERISTICS AND APPLIED VOLTAGE

As shown in figure10, for the small voltage V less than V_0 the gas discharge doesn't occur and the oxygen gas is

an insulator; meanwhile, the concentrations of all categories of charged particles are zero and $j_{total} = 0$. In the applied voltage range from V_0 to $2.1V_0$, the current density begins increasing relatively slightly with applied voltages; for $V \geq 2.1V_0$, the j_{total} grows quickly. The form of the characteristic curve of I-V in our theory is in accordance with the finding of previous researches [14], [15], [25].
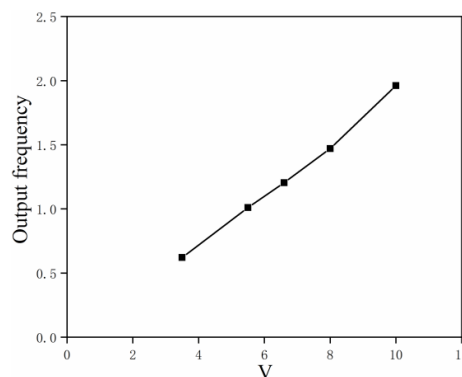
FIGURE 11. The changing curve of output frequency vs. applied voltage.

In particular, as seen in Fig.11, it is found that with rising applied voltage the pulsed frequency of output of j_{total} increases nearly linearly, which is in consistency with the results of previous researches as well [14], [17].
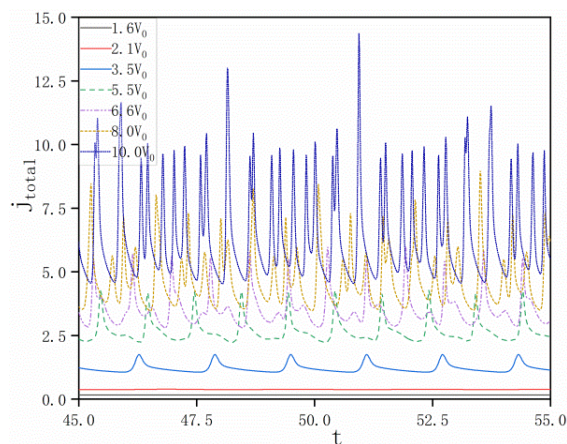
FIGURE 12. Output forms of the total current density waveforms for the following applied voltages: 1.6 V_0 (black full line), 2.1 V_0 (red full line), 3.5 V_0 (blue broken line), 5.5 V_0 (green broken line with short dashes), 6.6 V_0 (purple chain line with short dashes and dots), 8.0 V_0 (brown dotted line) and 10.0V_0(dark blue broken line).

2) DISCUSSION OF CURRENT DENSITIES j_{total}, j^- AND j^+: EVOLUTIONS WITH TIME AND VARIATIONS WITH APPLIED VOLTAGE

a: j_{total}

Fig. 12 depicts the change of the total current density j_{total} with time under different applied voltages. As seen in Fig. 12, for lower voltages 1.6V_0 and 2.1V_0 the positive corona has a quasi-stationary-state discharge current density which is

relatively small. When the voltage being raised to 3.5 V_0, the periodic discharge starts occurring and the slight and regular Trichel pulses are produced. Keeping the voltage increased to 5.5 V_0, the Trichel pulse becomes strong and slightly irregular. For voltages 3.5 V_0 and 5.5 V_0, the discharging current is periodic or quasi-periodic. When the voltage arrives to 6.6 V_0, the aperiodic discharge begins clearly occurring and moreover the Trichel pulse shows stronger and more irregular. Maintaining the voltage rising to 8.0 V_0, there is an obviously chaotic characteristic of discharge current density and the Trichel pulse becomes intensive, sharper and more very irregular. Especially, for the voltage $10V_0$, Trichel pulses of the current density are more intensive and have an extremely high frequency and greatly large amplitudes, which shows a strongly chaotic characteristic of positive corona discharge.

Noticeably, in different phases including periodic waves and chaotic waves, Trichel pulse displays a fast rising edge and a slowly falling edge with asymmetric stabbed form. The irregularly aperiodic outputs of Trichel pulses given in our theory are analogous to the previous experimental observations, as seen in Fig. 12. Although there are the same findings on the shapes of pulses in previous researches [14], [17], [15], [25], there are rarely theoretical predictions on the chaotic outputs for the positive corona discharge. Especially for the irregularly and asymmetrically jagged-like pulse of current density, the chaotic current output pattern in our research is qualitatively consistent with the corresponding results in previous literatures [2], [22].

The above case reveals that with the increase of voltage the positive corona has the higher discharge current and moreover Trichel pulses possess the more obviously chaotic form, higher frequency of oscillation and bigger amplitudes. In particular, as shown in Fig. 12, this nonlinear model in our theory can sufficiently predict three phases of positive corona discharge with the evolution of time as follows: the stationary discharge, the periodic discharge and the chaotic discharge.

b: j^+

As shown in Fig. 13, the positive ion current density as the component of total current density has the stationary or oscillatory pattern of output as well. For smaller applied voltage $1.6V_0$ and $2.1V_0$, the positive ion current density has stationary outputs with time. When the voltage rises to $3.5V_0$ and $5.5V_0$, the positive ion has the periodic pulsed outputs with the evolution of time. As the voltage rises to $6.6V_0$, the pulses of positive ion are not strictly periodic and begin showing slight aperiodic. When the voltage reaches to $8.0V_0$ and $10V_0$, the pulses with the evolution of time are no longer periodic and display strongly chaotic. In addition, it can be observed in Fig.13 that the positive current density rises fast and declines slowly in each pulse, which resembles the result of total current density but differs on the waveform of time series.
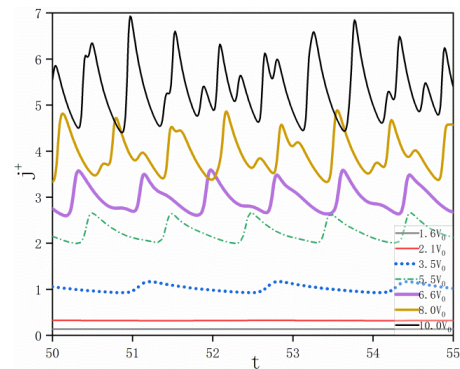

FIGURE 13. Output forms of the current density waveforms of positive ion for the following applied voltages: 1.6 V_0 (gray full line), 2.1 V_0 (red full line), 3.5 V_0 (blue dotted line), 5.5 V_0 (green chain line with short dashes and dots), 6.6 V_0 (purple full line), 8.0 V_0 (brown full line) and 10.0V_0 (black full line).
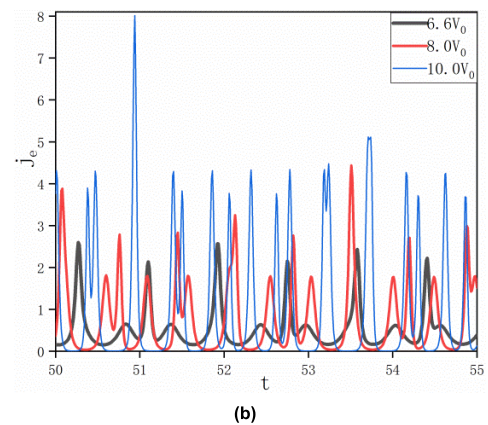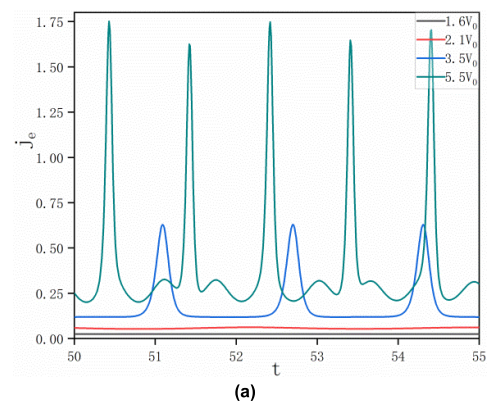

(a)

(b)

FIGURE 14. (a). Output forms of the electron current density waveforms for the following applied voltages: 1.6 V_0 (gray full line), 3.5 V_0 (blue full line), and 5.5 V_0 (green full line). (b). Output forms for the following applied voltages 6.6 V_0 (black full line), 8.0 V_0 (dark red full line) and 10.0 V_0(blue full line).

c: j_e

About the electron current density j_e seen in Fig. 14(a) and 14(b), for lower voltages $1.6V_0$ and $2.1V_0$ there is a quasi-stationary small current density of electrons. When the voltage is raised to 3.5 V_0 the current density of

electrons starts having regular and periodic pulses. For the higher applied voltage $5.5\ V_0$, the pulse becomes strong and slightly irregular. For lower voltages $3.5\ V_0$ and $5.5\ V_0$, it is found that the electronic current density has a periodic or quasi-periodic variation. When the applied voltage arrives to $6.6\ V_0$, the aperiodic wave obviously occurs and the pulse shows irregular. As setting the applied voltage to $8.0 V_0$ or $10 V_0$, the electronic current densities have apparently chaotic pulses with more sharp shapes and more irregular intervals between pulses. Especially, for the voltage $10\ V_0$, the current density of electrons has intensively chaotic pulses with greatly high frequency and very large amplitudes, which means there is a very strong ionization on oxygen molecules.

Meanwhile for the oscillation output of electronic current density, it is also found that the pulses of electronic current density have a symmetric and steep shape, which differs from asymmetric shapes of the pulses of total current density and positive current density. What leads to this case? Since the mass of electron is negligibly small and the migration time in the discharge layer is very short, the pulsed form is hardly affected by the change of surface electric field.

d: j_i^-

As seen in Fig. 15(a) and 15(b), the current density of negative ions has the similar pattern of output to the current density of electrons. Nevertheless, the current density of negative ions is far less than that of electrons or positive ions and then is usually considered to be negligible, whether in periodic discharge or chaotic discharge. This case is also found in the research of Morrow [14].

By the discussion on different current densities, with the increase of voltage j_{total}, j^-, j_e and j^+ all experience three phases such as the stationary output, the periodic output and the chaotic output.

3) CONTRIBUTIONS OF VARIOUS CURRENT DENSITIES TO THE TOTAL CURRENT DENSITY

The total corona current density consists of three pulsed components because of the drift of electrons, positive and negative ions. For the periodic discharge at low voltage $3.5 V_0$, the contributions of various current densities to the total current density are shown in Fig. 15(a). Particularly, the biggest contribution to the total current density is given by the positive ion current density while the electron current density contributes a few to the total current density compared with the positive ion current density. Additionally, the current density of negative ions provides a negligibly little contribution. During periodic discharge, at the center in the pulse of total current density the contribution of positive current density to the total current density is much more than those of electron current density and negative ion current density. Meanwhile, even between pulses, the positive current density still has the main contribution but the contributions of electron current density and negative ion current density are nearly negligible. Furthermore, the contributions of diverse charged-particle
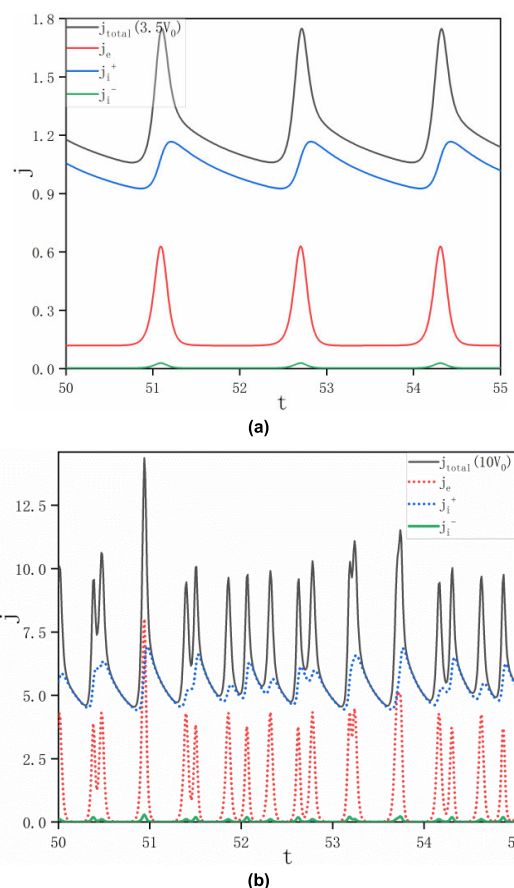

(a)

(b)

FIGURE 15. (a). For the onset voltage $3.5V_0$, the contributions of each species of charged particle current densities to the total current density in periodic Trichel pulses: the total current density (black full line), the positive ion density (blue full line), the electron current density (red full line) and the negative ion current density (green full line). (b). For the onset voltage $10V_0$, the contributions of each species of charged particle current densities to the total current density in chaotic Trichel pulses: the total positive current density (black full line), the positive ion density (blue dotted line), the electron current density (red dotted line) and the negative ion current density (green full line).

current densities to the total current density are consistent to the result in the research of Morrow [14].

Interestingly, even for the chaotic discharge at higher voltage $10V_0$ there is still a similar pattern of contributions of different current densities to the total current density except for a few peaks, as shown in Fig.15(b) although the current densities of positive ions, negative ions and electrons have respectively different chaotic pulsed waveform.

Especially, due to the most contribution to the total current density from the positive ion current density, the asymmetric shape of the total current density is decided mainly by the positive ion current density. Additionally, the contribution of electron ion current density leads to the spike-like waveform of total current density.

4) DISCUSSION OF CHARGED PARTICLES AND PHOTON
a: n_i^+

As is seen in Fig. 16, with the rise of applied voltage the number density of positive ions significantly increases and
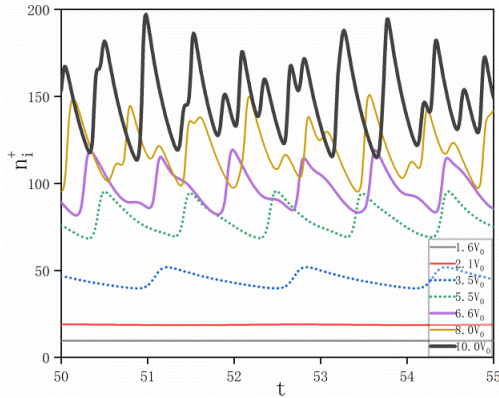
FIGURE 16. Output forms of the waveforms of positive ion number density for the following applied voltages: 1.6 V_0 (gray full line), 2.1 V_0 (red full line), 3.5 V_0 (blue dotted line), 5.5 V_0 (green dotted line), 6.6 V_0 (purple full line), 8.0 V_0 (brown full line) and 10.0V_0 (black full line).

meanwhile amplitudes and frequencies of wave become bigger and higher correspondingly. In general, the changes of positive ions separate into three phases. Under lower applied voltage, the positive ion has nonzero-stationary outputs. When the voltage rises to 3.5V_0 and 5.5V_0, the positive ion has the periodic pulses with the evolution of time. As the voltage rises to 6.6V_0, the pulses of positive ion are not strictly periodic and begin showing slight chaotic. Next, when the voltage is turned up to higher level 8.0V_0 and 10V_0 the pulses with the evolution of time are not periodic any longer and display strongly chaotic.

For positive ion number density and positive ion current density, because of the slow drift, long drift time and relatively big mass of positive ions, positive ions stay in the ionization region for a relative long time, relatively slowly move out of the discharge layer and are influenced obviously by the electric field. This results in a broad width of pulses and an asymmetric pulsed shape of steep rising and slowly falling edges.

b: n_e

Fig. 17(a) shows for low applied voltage 1.6V_0 there exists the output of constant number density of electrons with time. When the voltage increases to 2.1V_0, a very slight oscillation occurs. For the moderate voltage 3.5V_0, the electron number density has obviously periodic pulses. Keeping the voltage rising to 5.5V_0, the electron number density waves in stabbed pulses which are more sharp and obviously higher than that of 3.5V_0. In Fig. 17(b), for higher voltages 6.6, 8.0 and 10.0V_0 the electron number density has chaotic patterns of fluctuation. Generally speaking, with the rise of applied voltage the electron number density has more sharply stabbed pulses, higher frequencies and more chaotic oscillations.

c: n_{ph}

Fig. 18(a) and 18(b) illustrate the number density of photons has the correspondingly synchronous modes of output with the number density of electrons including the
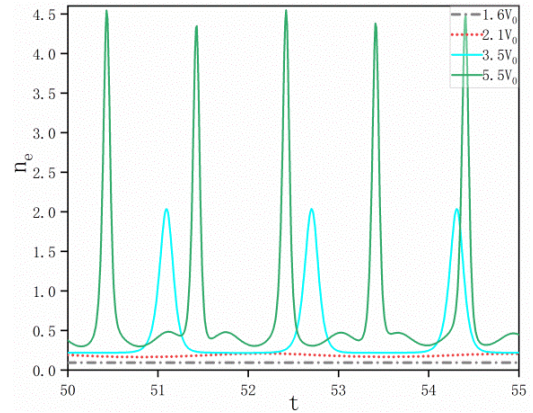
(a)
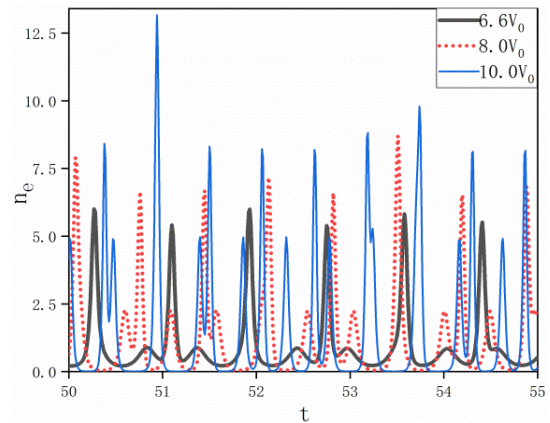
(b)

FIGURE 17. (a). Output forms of the waveforms of electron number density for the following applied voltages: 1.6 V_0 (gray chain line with short dashes and dots), 2.1 V_0 (red dotted line), 3.5 V_0 (light green full line) and 5.5 V_0 (green full line). (b). Output forms of the waveforms of electron number density for the following applied voltages: 6.6 V_0 (black full line), 8.0 V_0 (red dotted line) and 10.0V_0 (blue full line).

stationary-states, periodic-states and chaotic states. Especially under higher applied voltages the photon output displays the chaotic pulsed oscillation synchronized with the current oscillation.

Moreover, the output of photon number density as well as the output of electron number density has sharp saw-toothed pulses, which is very similar to the results in the previous theories [14]. These reflect the avalanche of electrons is simultaneously generated with the excitation radiation and the recombination radiation.

By comparison between the electron number density and the photon number density waveforms, it is found that for lower applied voltage there are very similar sharp periodic pulses of electron and photon number densities. In addition, when the ionization bursts, the electrons are generated rapidly and quickly reach the peak. In the meantime, by the excitation of metastable oxygen molecules and the recombination of positive ions and the electron, the photons are also quickly produced and instantly reach the peak. Besides, compared to positive ions, due to negligible mass of electron, zero mass
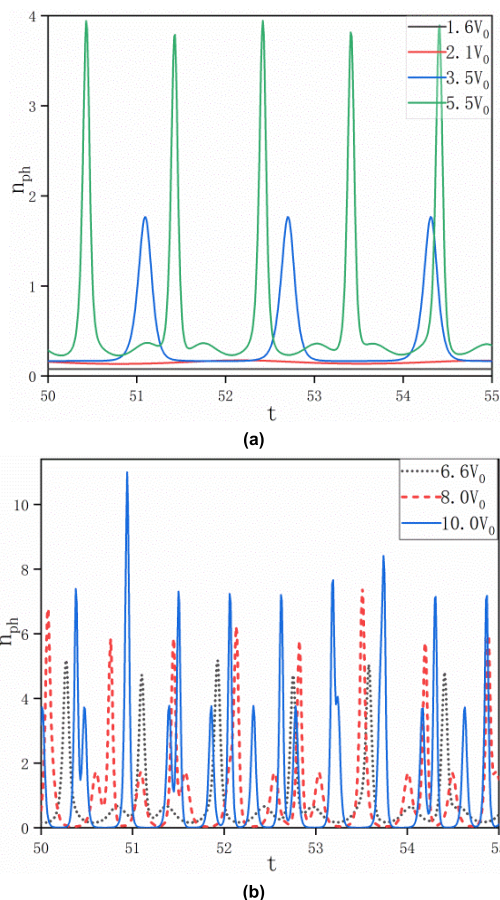
FIGURE 18. (a). Output forms of the waveforms of photon number density for the following applied voltages: 1.6 V_0 (gray full line), 2.1 V_0 (red full line), 3.5 V_0 (blue full line), 5.5 V_0 (green full line). (b). Output forms of the waveforms of photon number density for the following applied voltages: 6.6 V_0(black dotted line), 8.0 V_0 (red broken line with short dashes) and 10.0V_0 (blue full line).

FIGURE 19. (a). The waveform of positive ion number density at applied voltage 5.5 V_0. (b). The waveform of surface electric field strength at applied voltage 5.5V_0.

of photon and the very fast migration velocities of electrons and photons, electrons and photons hardly stay in the ionization region, rapidly move out of the discharge layer or are quickly absorbed by the anode and are barely influenced by the electric field. Consequently, these factors decide that electron and photon number densities both have a short burst of pulse, a narrow width of pulse and a symmetric or quasi-symmetric spike-like pulsed shape with the steep rising and falling edges. Likewise, for higher voltage the chaotic pulses of electron number density and photon number density also have the similar narrow pulsed width and the steep rising and falling edges although the pulses don't always retain a symmetric or quasi-symmetric shape.

5) THE PHYSIC RELATION BETWEEN POSITIVE ION NUMBER DENSITY n_i^+ AND SURFACE ELECTRIC FIELD STRENGTH E

As seen in Fig.19(a) and 19(b), it is found that the number density of positive ions with time evolution has a reverse oscillatory pattern to the strength of electric field (i.e. in each pulse, the number density of positive ion rises fast and declines slowly whereas the strength of electric field rises
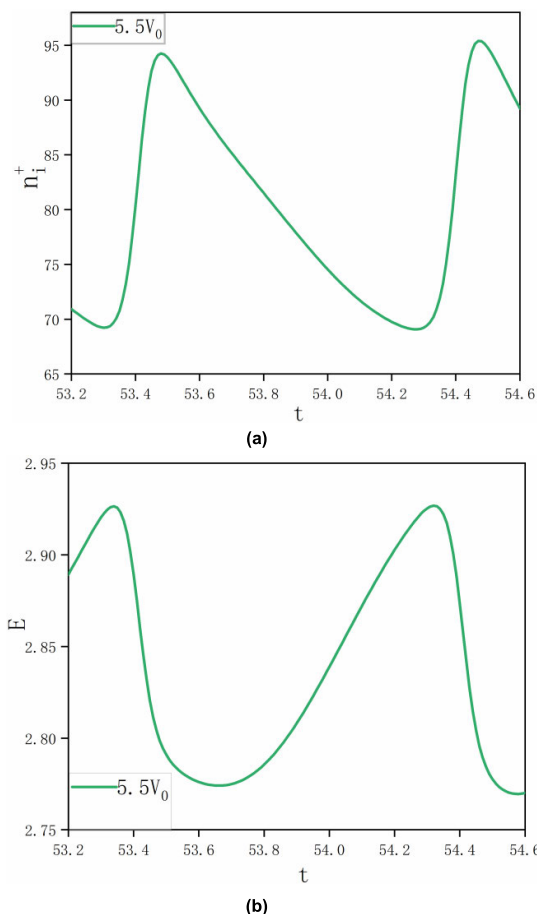
slowly and falls fast.). Due to the relatively big mass of positive ion, the long migration time and the slow ionic migration velocity, the electric field's influence on positive ions cannot be neglected, indicating the positive ions produced in per burst of ionization rely heavily on the change of electric field strength. Under the strong surface electric field, the oxygen molecules are rapidly ionized and the positive ion number density quickly attains the peak values, meaning the positive ions have a steep rising edge of pulse. As positive ions accumulate in the discharge layer, the surface electric field is impaired by the build-in electric field produced by the space electric charge accumulation. Thus, the ionization of oxygen molecules slows down under relatively weak surface electric field and the recombination of positive ions and electrons increases gradually, signifying the positive ions have a slowly falling edge of pulse. These lead to the asymmetric pulsed shape of positive ion number density.

For the surface electric filed, due to the slow migration speed of positive ions, the build-in electric field slowly decreases, which implies the surface electric field strength ascends slowly. When the surface electric field strength

gradually reaches to the peak, the oxygen molecules are rapidly ionized and thus the accumulation of space electric discharge quickly attains the maximum as well. In the meantime, the built-in electric field also reaches to the maximum. Then, the surface electric field is rapidly weakened by the strong built-in electric field produced by the quick accumulation of the space electric charge, which means the surface electric field strength descends fast. This is why the surface electric field strength has the reverse pulsed shape, namely an asymmetric pulse of slowly rising and fast falling edges.

According to the above discussions, it is figured out that the relatively big mass, slow migration speed and long migration time of positive ions are the main reason producing the asymmetric pulsed shapes and broad pulsed width of j_i^+ and n_i^+; meanwhile the pulsed shape of total current density is determined by the most contribution to the total current density offered by the drift of positive ions. However, for electrons of negligible mass and massless photons, due to the fast migration velocity, short migration time of electrons and photons and the negligible influence of electric field in the ionization region, n_e, n_{ph} and j_e have the short burst of pulse, the narrow pulsed width and the symmetric or quasi-symmetric pulsed shapes. Besides, the reverse waveform of surface electric field depends on the change of positive ions number density in the ionization region. Generally speaking, the pulsed shape and oscillatory patterns of particle number densities are in agreement with those of correspondingly respective current densities.

IV. CONCLUSION

Our research systematically investigate the discharge process of positive corona and the discharge natures. Furthermore, we in depth study the microscopic physical mechanism of positive corona discharge, and fully analyse the variations of outputs with time using nonlinear dynamics method. Although a few previous researches focus on the discharge phenomena of positive corona and give the description of stationary-state and periodic-pulsed outputs, the inherent physic mechanism causing photon-ionization isn't clearly explained and the dynamical description on irregular-pulsed discharge of positive corona isn't still provided. Particularly, we figure out the dynamical mechanism of chaotic phenomenon for the positive corona discharge and give a profound explanation. Moreover, we propose a novel dynamical model and predict different stages of discharge. The important results and findings are as follows:

1) we figure out that the photons produced by recombination of e and O_2^+ have the energy higher than the ionization energy of oxygen molecule and possess diverse frequencies because of various kinetic energies of free electrons participating in recombination reaction in the discharge layer.

2) In contrast with the ambiguous explanation on the photo-ionization in the previous researches, based on the quantum mechanics we improve the previous studies and present a physical mechanism causing the

photo-ionization: the high frequency photons from recombination radiation are functional to ionize neutral molecules producing the seed electrons and then triggering electron avalanches during the positive corona discharge due to the fact that the photons generated by the recombination have the higher energy than ionization energy of neutral oxygen molecules.

3) Meanwhile, we also point out that the energy of photons arisen from the radiation of metastable-ground energy level transition of O_2 molecules is less than the ionization energy of O_2 molecules and thus the excitation radiation is not capable to ionize O_2 generating the seed electrons in pure gas.

4) Our dynamical model can describe the Trichel pulse and the characteristics of waveforms, and predict the jagged-pulses of periodic outputs and ragged jagged-pulses of chaotic outputs and give the three phases. Especially the chaotic outputs of current is consistent to the actual observation of current pulses in experiments.

5) We preliminarily find out a dynamical mechanism producing the chaos: a chaotic system may be coupled by periodic oscillators. Meanwhile we discover the formation mechanism of irregular pulsed discharge on positive corona: for the positive corona discharge system, a chaotic discharge can be understood to be coupled by multiple different periodic discharge components which are caused by the various high-frequency photons.

6) Additionally, the further study finds the photons occurring can be mathematically treated as the feedback signal which plays a major role in the pulse discharge; the recombination term is canceled, namely that no photo-ionization appears, and then there exist no continuous pulses during discharge; essentially, the high frequency photons occurring is prepared for the next electron avalanche, namely for the next pulsed discharge. These reflect that our dynamical model agrees with the actual physical process of positive corona discharge.

7) It is found that the pulsed outputs of positive corona discharge show spike-like and the frequency and amplitude of pulse becomes high with the applied voltage rising. Besides, the characteristics changing curves of V-I and V-frequency are consistent to results of previous literatures.

8) During the periodic discharge or the chaotic discharge, at the center in the pulse of total current density the contribution of positive current density to the total current density is much more than those of electron current density and negative ion current density. Meanwhile, even between pulses the positive current density has the main contribution while the contribution of electron current density and negative ion current density is nearly negligible. Furthermore, the contributions of diverse charged-particle current densities to the total current density are consistent to the result in research of R. Morrow.

9) A clear explanation on the characteristic of the steep rising and slowly falling edges of Trichel pulse is given; we find that the asymmetric pulsed shape of the total current density is decided mostly by the contribution from the positive ions current density; additionally the contribution of electron current density leads to the spike-like waveform of total current density.

10) We analyze the characteristics of pulses of electron number density and the photon number density and explain the microscopic mechanism generating the symmetric or quasi-symmetric saw-toothed shape of pulses. In the meantime, we find the negligible or zero mass, fast migration velocity and short migration time of electron and photon lead to a short burst of pulse of electron or photon number density, a narrow width of pulse and a symmetric or quasi-symmetric spike-like shape of pulse.

11) It is discovered that the slow drift, long drift time and relatively big mass of positive ion are the main reason causing a broad width of pulses and an asymmetric pulsed shape of positive ion number density and positive ion current density with steep rising and slowly falling edges. Moreover, it is demonstrated that the pulsed characteristic of total current density is determined mainly by drifting positive ions in the electric field.

12) It is found that the strength of surface electric field shows a reverse oscillatory pattern to the number density of positive ions (i.e. the surface electric field strength has a pulse with slowly rising and rapidly falling edges.). Meanwhile, we explain the interactional relation among the positive ions, built-in field and surface electric field.

Seeing that in microscopic level few theoretical researches on chaotic discharge mechanism have been done, our dynamical nonlinear model provides a method to investigate the chaotic discharge phenomenon of positive corona. Furthermore, in this paper a microscopic physical mechanism is proposed to explain the aperiodic discharge phenomenon of positive corona. This intrinsic knowledge of the discharge phenomena of positive corona is the preparation for the guidance on experiments and application of positive corona discharge.

REFERENCES

[1] M. Faraday, *Experimental Researches in Electricity*. New York, NY, USA: Dover, 1965, pp. 20–106.

[2] G. W. Trichel, "The mechanism of the positive point to plane corona near onset," *Phys. Rev.*, vol. 55, pp. 382–390, Feb. 1939.

[3] G. W. Trichel, "The mechanism of the negative point to plane corona near onset," *Phys. Rev.*, vol. 54, pp. 1078–1084, Dec. 1938.

[4] W. N. English, "Positive and negative point-to-plane corona in air," *Phys. Rev.*, vol. 74, no. 2, pp. 170–178, Jul. 1948.

[5] W. L. Lama and C. F. Gallo, "Systematic study of the electrical characteristics of the 'Trichel' current pulses from negative needle-to-plane coronas," *J. Appl. Phys.*, vol. 45, no. 1, pp. 103–113, Jan. 1974.

[6] C. Mayoux and M. Goldman, "Partial discharges in solid dielectrics and corona discharge phenomena," *J. Appl. Phys.*, vol. 44, pp. 3940–3994, Sep. 1973.

[7] G. F. L. Ferreira, O. N. Oliveira, and J. A. Giacometti, "Point-to-plane corona: Current-voltage characteristics for positive and negative polarity with evidence of an electronic component," *J. Appl. Phys.*, vol. 59, no. 9, pp. 3045–3049, May 1986.

[8] R. J. Van Brunt and D. Leep, "Characterization of point-plane corona pulses in SF_6," *J. Appl. Phys.*, vol. 52, no. 11, pp. 6588–6600, Nov. 1981.

[9] R. Ono, Y. Nakagawa, and T. Oda, "Effect of pulse width on the production of radicals and excited species in a pulsed positive corona discharge," *J. Phys. D, Appl. Phys.*, vol. 44, Dec. 2011, Art. no. 485201.

[10] A. S. Denholm, "The pulses and radio influence voltage of power-frequency corona," *Trans. Amer. Inst. Electr. Eng. III, Power App. Syst.*, vol. 79, no. 3, pp. 698–706, Apr. 1960.

[11] B. Rakoshdas, "Pulses and radio-influence voltage of direct-voltage corona," *IEEE Trans. Power App. Syst.*, vol. PAS-83, no. 5, pp. 483–491, May 1964.

[12] M. P. Sarma and W. Janischewskyj, "D.C. corona on smooth conductors in air. Steady-state analysis of the ionisation layer," *Proc. Inst. Elect. Eng.*, vol. 116, no. 1, pp. 161–166, 1969.

[13] T. Giao and J. Jordan, "Modes of corona discharges in air," *IEEE Trans. Power App. Syst.*, vol. PAS-87, no. 5, pp. 1207–1215, May 1968.

[14] R. Morrow, "The theory of positive glow corona," *J. Phys. D, Appl. Phys.*, vol. 30, no. 22, pp. 3099–3114, Nov. 1997.

[15] Y. S. Akishev, M. E. Grushin, A. A. Deryugin, A. P. Napartovich, M. V. Pan'kin, and N. I. Trushkin, "Self-oscillations of a positive corona in nitrogen," *J. Phys. D, Appl. Phys.*, vol. 32, no. 18, pp. 2399–2409, Sep. 1999.

[16] K. Adamiak, V. Atrazhev, and P. Atten, "Corona discharge in the hyperbolic point-plane configuration: Direct ionisation criterion versus approximate formulations," *IEEE Trans. Dielectr. Electr. Insul.*, vol. 12, no. 5, pp. 1015–1024, Nov. 2005.

[17] P. Dordizadeh, K. Adamiak, and G. S. Peter Castle, "Study of the impact of photoionization on negative and positive needle-plane corona discharge in atmospheric air," *Plasma Sources Sci. Technol.*, vol. 25, no. 6, Oct. 2016, Art. no. 065009.

[18] P. Sattari, C. F. Gallo, G. S. P. Castle, and K. Adamiak, "Trichel pulse characteristics—Negative corona discharge in air," *J. Phys. D, Appl. Phys.*, vol. 44, Apr. 2011, Art. no. 155502.

[19] T. N. Tran, I. O. Golosnoy, P. L. Lewin, and G. E. Georghiou, "Numerical modelling of negative discharges in air with experimental validation," *J. Phys. D, Appl. Phys.*, vol. 44, no. 1, Jan. 2011, Art. no. 015203.

[20] F. C. Deng, L. Y. Ye, and K. C. Song, "Numerical studies of Trichel pulses in airflows," *J. Phys. D, Appl. Phys.*, vol. 46, no. 42, Sep. 2013, Art. no. 425202.

[21] N. C. Sung, "Physics of self-sustained oscillations in the positive glow corona," *Phys. Plasma*, vol. 19, pp. 1353–1362, Jul. 2012.

[22] D. W. Lamb, "Optical studies of positive coronas in air," Ph.D. dissertation, Dept. Appl. Phys., New England Univ., Armidale, NSW, Australia, 1992.

[23] G. W. Penney and G. T. Hummert, "Photoionization measurements in air, oxygen and nitrogen," *J. Appl. Phys.*, vol. 41, pp. 572–577, Feb. 1970.

[24] G. V. Naidis, "On photoionization produced by discharges in air," *Plasma Sources Sci. Technol.*, vol. 15, no. 2, pp. 253–255, May 2006.

[25] L. Liu and M. Becerra, "An efficient model to simulate stable glow corona discharges and their transition into streamers," *J. Phys. D, Appl. Phys.*, vol. 50, no. 10, Feb. 2017, Art. no. 105204.

[26] S. H. Strogatz, *Nonlinear Dynamics and Chaos: With Applications to Physics, Biology, Chemistry, and Engineering*. Boulder, CO, USA: Westview Press, 2014, pp. 230–506.

[27] A. Fuchs, *Nonlinear Dynamics in Complex Systems: Theory and Applications for the Life-, Neuro- and Natural Sciences*. New York, NY, USA: Springer, 2013, pp. 3–87.

[28] J. M. T. Thompson, *Nonlinear Dynamics and Chaos*. Hoboken, NJ, USA: Wiley, 1986, pp. 205–226.

[29] S. Sastry, *Nonlinear Systems: Analysis, Stability, and Control*. New York, NY, USA: Springer, 1999, pp. 31–168.

[30] R. D. Janz, D. J. Vanecek, and R. J. Field, "Composite double oscillation in a modified version of the oregonator model of the Belousov–Zhabotinsky reaction," *J. Chem. Phys.*, vol. 73, no. 7, pp. 3132–3138, Oct. 1980.

[31] W. Jahnke, W. E. Skaggs, and A. T. Winfree, "Chemical vortex dynamics in the Belousov–Zhabotinskii reaction and in the two-variable oregonator model," *J. Phys. Chem.*, vol. 93, no. 2, pp. 740–749, Jan. 1989.

PANLONG AN received the Ph.D. degree from the North University of China, in 2015. He is currently an Associate Professor with the Shaanxi Railway Institute. His research interests include MOEMS systems and advanced optical sensors.

JIAN SUI received the Ph.D. degree in the condensed matter physics from Chongqing University, in 2014. Since 2014, he has been working in the theoretical research of ultra high voltage discharge with the State Key Laboratory of Power Transmission Equipment and System Security and New Technology, Chongqing University. His research interests include nonlinear phenomena of corona discharge and microscopic mechanism of weakly ionized plasma discharge.

ZHENGGUANG LIU received the Ph.D. degree in material physics and chemistry, in 2014. He has been working for ten years at the North University of China, since 2005. Currently, he works at Zhaoqing Medical College. His research interests include electronics and ab initio theory.

● ● ●